Classification of Edge-to-edge Monohedral Tilings of the Sphere

Ho Man Cheung*[1], Hoi Ping Luk†[2], and Min Yan‡[3]

[1,2,3]The Hong Kong University of Science & Technology, Hong Kong.

Abstract

The history of studies on tilings of the sphere can be traced back to Plato (5 Platonic solids) and Archimedes (13 Archimedean solids). We study edge-to-edge monohedral tilings of the sphere. The classification of such tilings was pioneered by D. Sommerville in 1923. Significant progress was made in the past decades. However, the remaining cases have been the most difficult to classify. They are also of the utmost importance as they give rise to the majority of the tilings. We have recently classified all of them and hence completed the whole classification celebrating its centenary. The process involved new techniques ranging from combinatorics, geometry, algebra and number theory. All the tilings can be classified into 3 types: Platonic type, earth map type, and sporadic type. The full classification gives us a comprehensive understanding of their structural relations.

1 Introduction

The *tilings* in our studies cover the surface of the sphere without holes and overlaps. A tiling is *monohedral* if all tiles are geometrically congruent to a fixed polygon. The polygon, assumed to have geodesic arcs as edges, is called the *prototile*. By [8, Lemma 1], the prototile of a monohedral tiling of the sphere must be simple, i.e., its boundary is a simple closed curve. The tilings are also *edge-to-edge*, which means that no vertex of a tile lies in the interior of an edge of another tile (for example, see Figure 1). We also assume that *the degree* of a vertex in a tiling is at least 3 to avoid trivial examples by artificially adding extra vertices to edges and the complications inflicted by that. For simplicity, by *tiling* we mean edge-to-edge monohedral tiling of the sphere satisfying the above assumptions.

Figure 1: Edge-to-edge v.s. non-edge-to-edge

By [11, Proposition 4], the prototile in a tiling is either a triangle, a quadrilateral, or a pentagon. We call the prototiles resulting in tilings the *admissible prototiles*. From [4, 10] and [12], they are shown in Figure 2) with notations for their edge combinations. For example, a^4b means 4 a-edges and 1 b-edge in a pentagon. Edges with different labels are assumed to have different lengths. In a^4, the notation $\bullet$ (and $\circ$) denotes the opposite angles of equal value, and $\bullet$ will be used in Figures 5 and 7.

D. Sommerville [9] first studied the tilings with triangle prototiles in 1923. H. L. Davies gave an outline for the classification [6], which was completed by Y. Ueno and Y. Agaoka [10] in 2002. H. H. Gao, N. Shi and M. Yan [8] classified the minimal case for pentagon prototiles in 2013 and significant progress has since been made by Y. Akama, E. X. Wang and M. Yan [1, 2, 12, 13] in the quadrilateral and the pentagon direction. The remaining and the hardest problems have prototiles with edge combinations a^2bc, a^3b and a^4b. By overcoming these challenges [3, 4, 5], we present the main result below.

*Email: hmcheungae@connect.ust.hk.

†Email: hoi@connect.ust.hk. Author was supported in part by the Li Po Chun Charitable Trust Fund scholarship.

‡Email: mamyan@ust.hk. Research was supported by Hong Kong RGC General Research Fund 16303515 and 16305920.

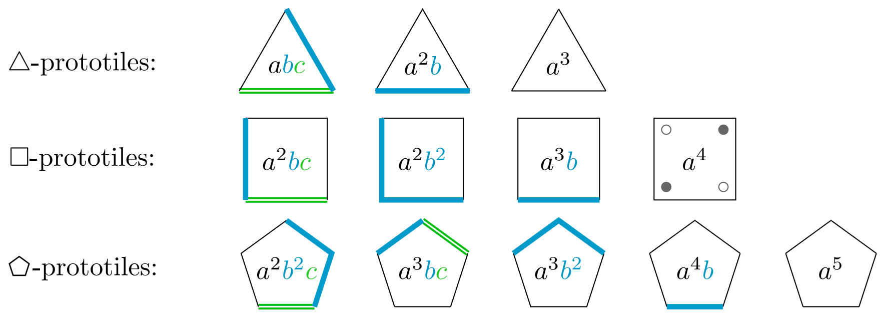

Figure 2: The admissible prototiles

2 Main result

Theorem 1. *The edge-to-edge monohedral tilings of the sphere are*

1. *Platonic type: Platonic solids* $P_* = P_4, P_6, P_8, P_{12}, P_{20}$ *and subdivisions on* P_* *below*
   - *Simple subdivision* S_iP_6 *of the cube for* $i = 1, ..., 7$*;*
   - *Triangular subdivision* TP_**;*
   - *Barycentric subdivision* BP_**;*
   - *Quadrilateral subdivision* QP_**;*
   - *Quadricentric subdivision* CP_**;*
   - *Pentagonal subdivision* PP_**;*
   - *Double pentagonal subdivision* DP_**;*
2. *Earth map type:*
   - 3 *infinite families of* $\triangle$*-tilings:* $E_\triangle 1$ *(with reductions* $E^I_\triangle 1, E^J_\triangle 1$*),* $E_\triangle 2$ *and* $E_\triangle 3$*;*
   - 2 *infinite families of* $\square$*-tilings:* $E_\square 1$ *(with reductions* $E^A_\square 1, E^K_\square 1, E^R_\square 1$*) and* $E_\square 2$*;*
   - 2 *infinite families of* $\pentagon$*-tilings:* $E_{\pentagon} 1$ *and* $E_{\pentagon} 2$*;*
3. *Sporadic type:* $S_{12\square}1, S_{16\square}1, S_{16\square}2, S_{16\square}3($*and* $FS_{16\square}3), S_{16\square}4, S_{36\square}5, S_{36\square}6, S_{16\pentagon}$*;*
4. *Modifications:*
   - *Flip* F*:*
     Platonic - $FBP_8, FQP_6, FQP_8, FPP_8, F_1PP_{20}, F_2PP_{20}$*;*
     Earth map $\triangle$*-tilings -* $FE_\triangle i$ *where* $i = 1, 2, 3$*;*
     Earth map $\square$*-tilings -* $FE_\square 1, F_1E_\square 2, F_2E_\square 2$*;*
     Earth map $\pentagon$*-tilings -* $F_1E_{\pentagon} i, F_2E_{\pentagon} i$ *for* $i = 1, 2$*, and* $F'_2E_{\pentagon} 2, F''_2E_{\pentagon} 2$*;*
     Sporadic - $FS_{16\square}3$*;*
   - *Rearrangement* R*:* $RE_\square 1$*.*

The distinguishing features of tilings are best demonstrated in plane drawings. Platonic type tilings are shown in Figures 3, 4, 5 and 6, where the open ends of the outmost edges in a drawing converge to a single vertex. Earth map type tilings are shown in Figures 7 and 8, where the vertical edges in the top row of each drawing converge to a vertex (the "north pole") and those in the bottom converge to another (the "south pole"), and the left and right boundaries are identified. Sporadic tilings are shown in Figures 9 and 10. Two examples of modifications on QP_8 and on $E^A_\square 1$ are shown respectively in Figures 11 and 12. The readers are referred to [4] and [5] for detailed discussion on modifications, including the most sophisticated ones.

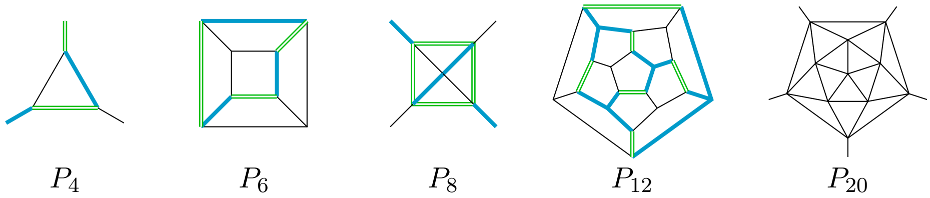

Figure 3: Platonic solids

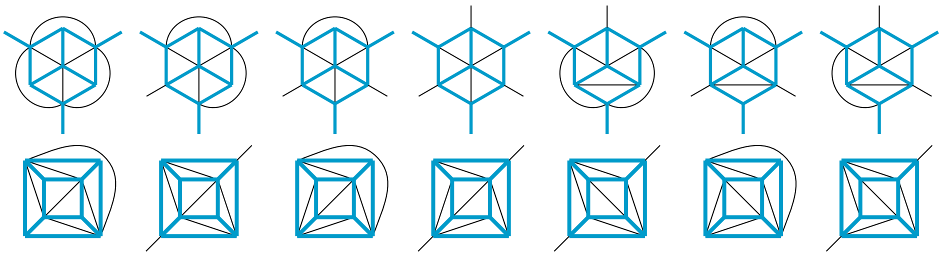

Figure 4: Simple triangular subdivisions of the cube P_6

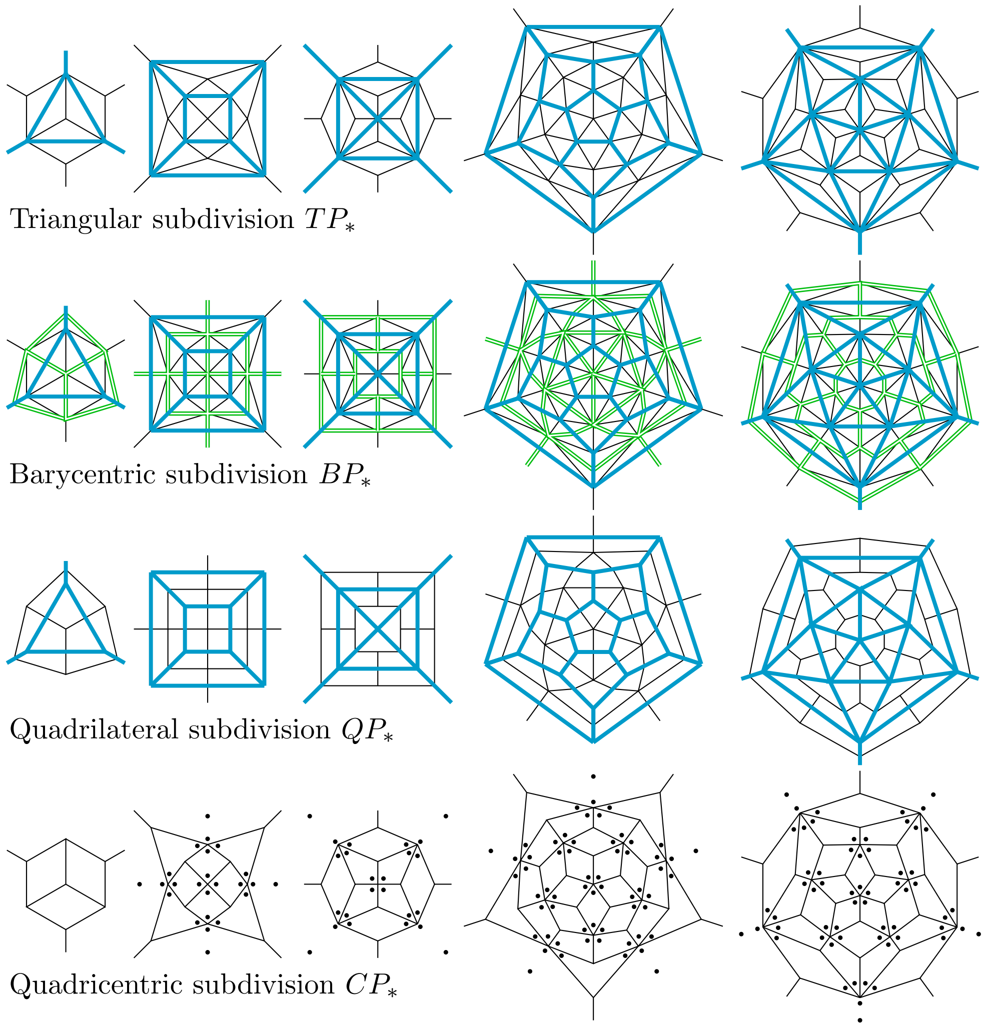

Figure 5: Subdivisions of Platonic solids TP_*, QP_*, BP_*, and CP_*

We highlight some interesting facts before the sketch of the proof. First, P_{20} is the only Platonic

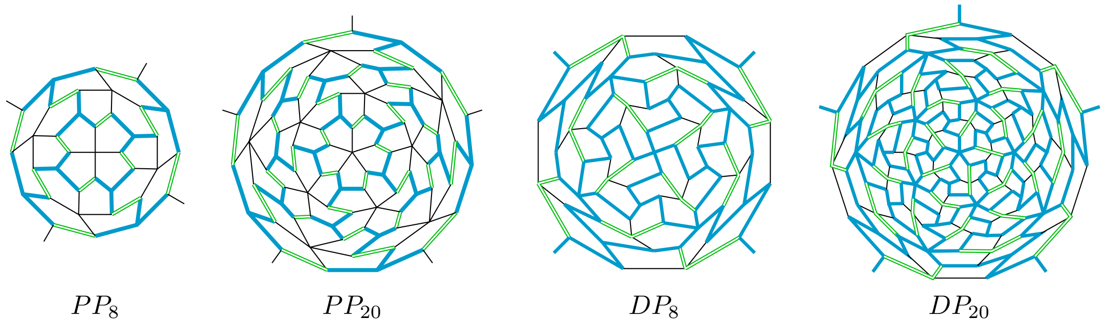

Figure 6: Pentagonal subdivisions and double pentagonal subdivisions of P_8 and P_{20}

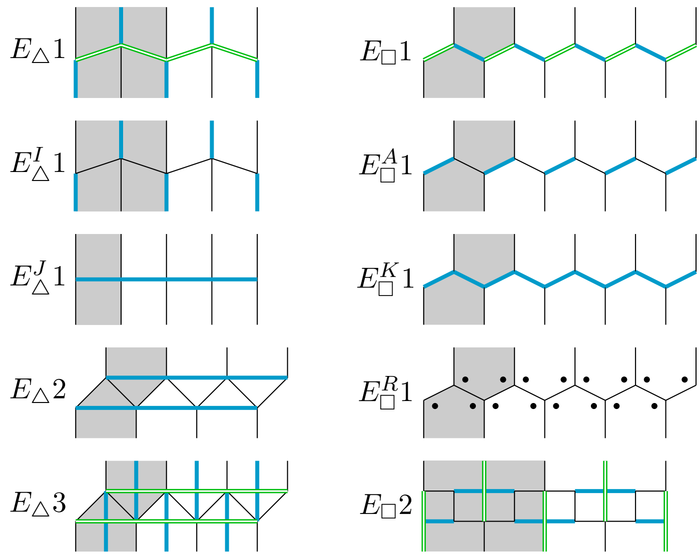

Figure 7: Earth map type △-tilings and □-tilings

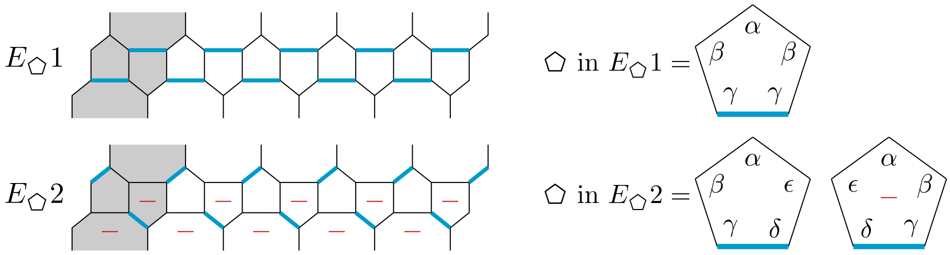

Figure 8: Earth map type ⬠-tilings

solid that gives a rigid tiling. Second, the earth map type tilings (or earth map tilings) resemble the earth map – hence the name. Notably, the poles of earth map tilings are the vertices with negative combinatorial curvature (see definition in [7]). Between them, a tiling is formed by repeating copies of *a timezone* (shaded). Third, in $S_{16\square}3$ and $FS_{16\square}3$, one angle is actually π. Hence they are also non-edge-to-edge △-tilings.

Sketch of proof. The complete classification is obtained by determining

1. the admissible prototiles, and

2. the corresponding admissible vertices in terms of angle combinations for each admissible prototile.

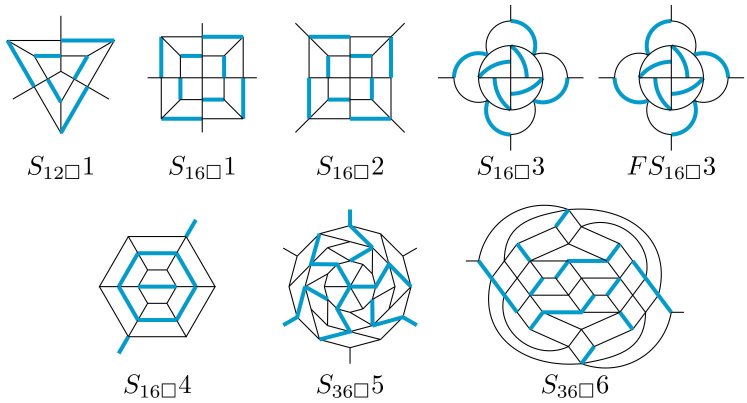

Figure 9: Sporadic $\square$-tilings $S_{12\square}1, S_{16\square}1, S_{16\square}2, S_{16\square}3, FS_{16\square}3, S_{16\square}4, S_{36\square}5, S_{36\square}6$

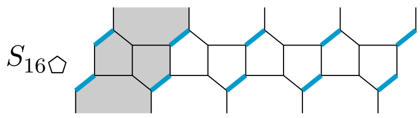

Figure 10: The sporadic $\pentagon$-tiling $S_{16\pentagon}$

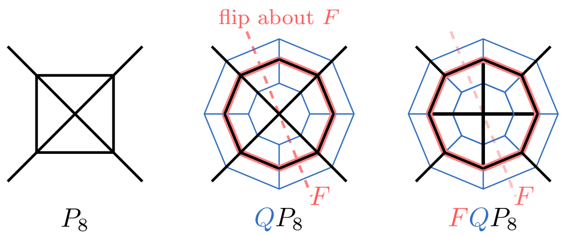

Figure 11: Platonic type tiling from subdivision to modification: $P_8 \to QP_8 \to FQP_8$

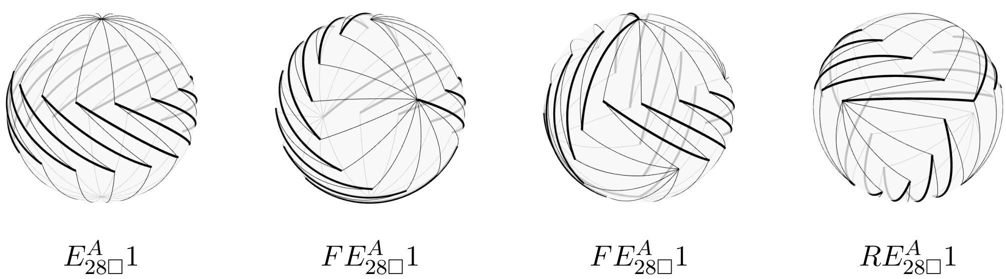

Figure 12: An example of modifications – earth map tiling $E^A_{28\square}1$, two tilings from flip modification $FE^A_{28\square}1$ and a rearrangement $RE^A_{28\square}1$

Such a set of vertices satisfies various combinatorial and geometric contraints. We call it *anglewise-vertex combination* (or AVC for short). The tiling in the first picture of Figure 13 has AVC $= \{\alpha\gamma\delta, \beta^n\}$.

The knowledge of AVC is pivotal: it serves as the instruction of how to put the tiles together. For example, suppose that we have AVC $= \{\alpha\gamma\delta, \beta^3\}$ for the prototile a^3b. Then every vertex is $\alpha\gamma\delta$ or β^3. The notation $\alpha\gamma\delta$ means that a vertex has one α, one γ and one δ (see first picture, Figure 13) whereas β^3 means that a vertex has three β's. In the second picture, a vertex $\alpha\gamma\delta$ uniquely determines the three incident tiles ①,②,③. Similarly, we then determine $\alpha_3\gamma_1\cdots = \alpha\gamma\delta$ and $\gamma_3\delta_2\cdots = \alpha\gamma\delta$ and $\beta_3\cdots, \beta_1\beta_2\cdots = \beta^3$. Repeating such process, we uniquely determine the tiling given by the cube P_6 in the third picture. The same argument works for AVC $= \{\alpha\gamma\delta, \beta^n\}$ with any fixed integer $n \geq 3$. The tiling obtained is indeed $E^A_\square 1$ in the first picture where $n = 3$ gives P_6 (shaded).

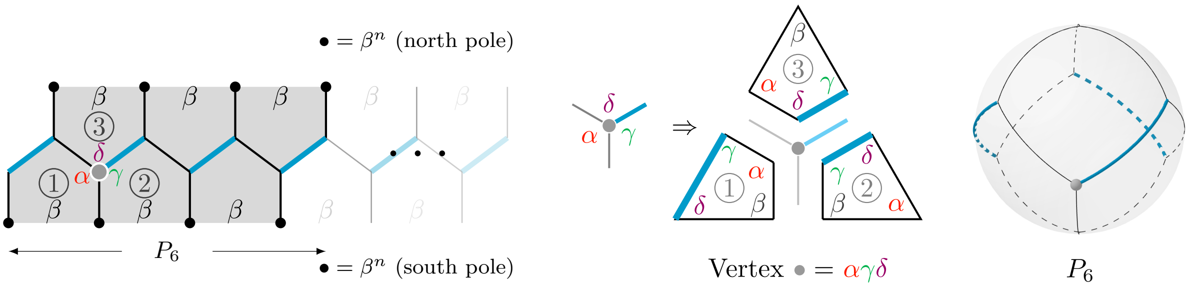

Figure 13: Construction of the tiling $E_\square 1$ with prototile a^3b and AVC $= \{\alpha\gamma\delta, \beta^n\}$

By edge configurations and the existence of vertices of certain degrees, we obtain the prototiles in Figure 2. See [4, Lemma 1] and [12, Lemma 9] for further details.

For each admissible prototile, it takes both combinatorial and geometric arguments to determine the AVCs. It boils down to the study of the angles in a tiling. Powerful tools, such as discharging method, convexity analysis, spherical trigonometry, Gröbner basis, trigonometric Diophantine analysis and integer linear programming, are implemented for this purpose. $\square$

The full classification of the △-tilings can be see in [4, 10], the full classification of the □-tilings can be seen in [4], and the full classification of ⬠-tilings is the collective effort of [1, 2, 5, 8, 12, 13]. An alternative classification of tilings with a^3b prototile via a noval approach is given in [3].

References

[1] Y. Akama, E. X. Wang, M. Yan, Tilings of the sphere by congruent pentagons III: edge combination a^5, *Adv. in Math.* **394** (2022), #107881.

[2] Y. Akama, M. Yan, On deformed dodecahedron tiling, *Australas. J. of Comb.* **85(1)** (2023), 1–14.

[3] H. P. Luk, H. M. Cheung, Rational angles and tilings of the sphere by congruent quadrilaterals, *Ann. Comb.* **28** (2024), 485–527.

[4] H. M. Cheung, H. P. Luk, M. Yan, Tilings of the sphere by congruent quadrilaterals or triangles, *preprint*, 2022, `arXiv:2204.02736`.

[5] H. M. Cheung, H. P. Luk, M. Yan, Tilings of the sphere by congruent pentagons IV: edge combination a^4b, *preprint*, 2023, `arXiv:2307.11453`.

[6] H. L. Davies, Packings of spherical triangles and tetrahedra, *Proceedings of the Colloquium on Convexity* **ed. W. Fenchel** (1967), Københavns Univ. Mat. Inst., Copenhagen, 42–51.

[7] Y. Higuchi, Combinatorial curvature for planar graphs, *J. Graph Theory* **38(4)** (2001), 220–229.

[8] H. H. Gao, N. Shi, M. Yan, Spherical tiling by 12 congruent pentagons, *J. Comb. Theory Ser. A* **120(4)** (2013), 744–776.

[9] D. M. Y. Sommerville, Division of space by congruent triangles and tetrahedra, *Proc. Royal Soc. Edinburgh* **43** (1923), 85–116.

[10] Y. Ueno, Y. Agaoka, Classification of tilings of the 2-dimensional sphere by congruent triangles, *Hiroshima Math. J.* **32(3)** (2002), 463–540.

[11] Y. Ueno, Y. Agaoka, Examples of spherical tilings by congruent quadrangles, *Math. Inform. Sci., Fac. Integrated Arts Sci., Hiroshima Univ.* **Ser. IV 27** (2001), 135–144.

[12] E. X. Wang, M. Yan, Tilings of sphere by congruent pentagons I: edge combinations a^2b^2c and a^3bc, *Adv. in Math.* **394** (2022), #107866.

[13] E. X. Wang, M. Yan, Tilings of sphere by congruent pentagons II: edge combination a^3b^2, *Adv. in Math.* **394** (2022), #107867.